Proteomic Analysis of Glycosylphosphatidylinositol-anchored Membrane Proteins*

Felix Elortza‡§, Thomas S. Nühse¶‖, Leonard J. Foster‡, Allan Stensballe‡, Scott C. Peck¶, and Ole N. Jensen‡ ‡‡**

Glycosylphosphatidylinositol-anchored proteins (GPI-APs) are a functionally and structurally diverse family of post-translationally modified membrane proteins found mostly in the outer leaflet of the plasma membrane in a variety of eukaryotic cells. Although the general role of GPI-APs remains unclear, they have attracted attention because they act as enzymes and receptors in cell adhesion, differentiation, and host-pathogen interactions. GPI-APs may represent potential diagnostic and therapeutic targets in humans and are interesting in plant biotechnology because of their key role in root development. We here present a general mass spectrometry-based proteomic "shave-and-conquer" strategy that specifically targets GPI-APs. Using a combination of biochemical methods, mass spectrometry, and computational sequence analysis we identified six GPI-APs in a *Homo sapiens* lipid raft-enriched fraction and 44 GPI-APs in an *Arabidopsis thaliana* membrane preparation, representing the largest experimental dataset of GPI-anchored proteins to date. ***Molecular & Cellular Proteomics 2: 1261–1270, 2003.***

Cell surface membrane proteins constitute an important class of biomolecules in living cells as they are in the interface with the surrounding environment. Most eukaryote membrane proteins are post-translationally modified, and a subset of these are modified by the covalent attachment of a glycosylphosphatidylinositol (GPI)[1] moiety at the C terminus of the protein (1). Anchoring to the lipid bilayer confers the GPI-anchored proteins (GPI-APs) a number of physicochemical properties that are shared with intrinsic plasma membrane proteins. GPI-APs act as surface coat proteins, receptors, adhesion molecules, ectoenzymes, differentiation antigens, and adaptors (2–5) and may also be involved in intracellular sorting and transmembrane signaling processes (6, 7). The lipidic part of the anchor has been shown to act as a signaling molecule, *e.g.* mammalian protein kinase C is activated by diacylglycerol (8).

GPI-anchored proteins are enriched in the sphingolipid- and cholesterol-enriched domains (lipid rafts) in mammalian cells (9) and possibly plant cells (10), but the number of GPI-anchored proteins that have been identified in individual proteomic studies of lipid raft preparations is still small and until this time has not exceeded five (11).

All known GPI-APs share a number of common features (12) including the absence of transmembrane domains, a cleavable N-terminal secretion signal for translocation into the endoplasmic reticulum, and a predominantly hydrophobic region in the C terminus, which most likely forms a transient transmembrane domain and functions as a recognition signal for a transamidase. The enzyme recognizes and processes the C-terminal hydrophobic tail of the nascent protein at the so-called "ω-site" and transfers the nascent protein to a presynthesized GPI anchor. Analysis of native GPI-APs and site-directed mutagenesis studies have shown that there are certain sequence constraints for the ω-site (13, 14). Based on such features, a number of bioinformatic methods for prediction of GPI-anchored proteins have been reported (16, 17).[2]

Computational methods provide a useful starting point for genome-wide screening of potential GPI-APs in a variety of model organisms. However, there is a growing need for the development of sensitive and general analytical methods for generation of experimental data to validate the *in silico* predictions and to study systematically the populations of GPI-APs at various stages of cellular development and differentiation, including pathogenic or perturbed states.

Arabidopsis thaliana is the model system of choice in plant cell biology. Mining of the *A. thaliana* genome sequence has led to the prediction of 248 putative GPI-APs (18). The modifying "machinery" appears to be conserved in plants (19), and

From the ‡Department of Biochemistry and Molecular Biology, University of Southern Denmark, Campusvej 55, DK-5230 Odense M, Denmark and ¶Sainsbury Laboratory, John Innes Centre, Norwich NR4 7UH, United Kingdom

Received, August 19, 2003, and in revised form, September 24, 2003

Published, MCP Papers in Press, September 29, 2003, DOI 10.1074/mcp.M300079-MCP200

[1] The abbreviations used are: GPI, glycosylphosphatidylinositol; GPI-AP, GPI-anchored protein; CRD, cross-reacting determinant; MS/MS, tandem mass spectrometry; HPLC, high performance liquid chromatography; MPSS, Massively Parallel Signature Sequencing; PI-PLC, phosphatidylinositol phospholipase C; MES, 4-morpholineethanesulfonic acid.

[2] J. Kronegg and D. Buloz, Detection/prediction of GPI cleavage site (GPI-anchor) in a protein (DGPI) at 129.194.185.165/dgpi/.

the structure of the GPI anchor is similar to that of other eukaryotes (20). Three genes encoding putative GPI-APs were found in mutant screens as regulators of cell expansion and root architecture: COBRA (21), SKU5 (22), and SOS5 (23); and proteomic analyses have biochemically confirmed the presence of multiple GPI-APs in *Nicotiana* and *Arabidopsis*, leading to the identification of up to 30 plant GPI-APs to date (18, 24–26).

We report the development and application of a general proteomic approach directed at selective isolation and identification of GPI-APs (27). Using the concept of "modification-specific proteomics" (28, 48), we have combined membrane protein fractionation methods with a GPI-AP-selective biochemical assay for enrichment of GPI-APs. Tandem mass spectrometry and computational tools were used for protein identification and assignment of GPI-APs. Six known human GPI-APs were found in a HeLa cell raft-enriched membrane preparation, and a total of 44 GPI-APs were identified in *A. thaliana*.

EXPERIMENTAL PROCEDURES

Preparation of Membranes—After serum starvation HeLa cells were lysed in 100 mM Na_2CO_3, pH 11.0, and mechanically disrupted by 10 strokes in a Dounce homogenizer and three 20-s bursts of a probe sonicator. The lysates were clarified and combined with an equal volume of 90% sucrose in MES-buffered saline (MBS) (150 mM NaCl, 25 mM MES, pH 6.5) for a final sucrose concentration of 45%. This solution was then placed in the bottom of an ultracentrifuge tube as the base of a discontinuous sucrose gradient. Additional layers consisting of 35 and 5% sucrose in MBS were gently placed on top, and the whole gradient was centrifuged at 166,000 × *g* for 18 h at 4 °C. The resulting low density light-scattering band (~18% sucrose) was extracted, diluted 4× in Na_2CO_3, and centrifuged for a further 2 h (166,000 × *g*, 4 °C) to pellet the raft-enriched membranes (REM) (11, 30).

Suspension cultures of *A. thaliana* were maintained as described previously (31). Plasma membranes were prepared as reported (32) using a homogenization buffer containing 250 mM sucrose, 100 mM HEPES/KOH, pH 7.5, 15 mM EGTA, 5% glycerol, 0.5% polyvinylpyrrolidone K 25, 3 mM dithiothreitol, and 1 mM phenylmethylsulfonyl fluoride at 2 ml/g of fresh weight. Microsomal membranes were resuspended in buffer R (250 mM sucrose, 5 mM potassium phosphate, pH 7.5, 6 mM KCl) and subjected to phase partitioning (32) in 6.0% each dextran T-500 and polyethylene glycol 3350 in buffer R. For removal of external soluble proteins, plasma membranes were washed with 100 mM Na_2CO_3.

Two-phase Separation and Phosphatidylinositol Phospholipase C Treatment—Two-phase separation was performed based on the work of Bordier (33). Membranes were equilibrated by resuspending the pellet in buffer A (20 mM Hepes, pH 7.5, 0.2 mM phenylmethylsulfonyl fluoride, and 0.5 tablet of protease inhibitor/ml) and were pelleted again at 20,000 × *g* for 20 min. The membrane fraction was resuspended in 100 μl of buffer A, and then the same volume of Triton X-114 was added and mixed to homogeneity. The mixture was chilled on ice for 5 min and then transferred to 37 °C for 20 min for phase separation. The aqueous supernatant was discarded, and the procedure was repeated. The detergent phase was recovered, and 100 μl of buffer A with 2 units of PI-PLC (Molecular Probes Inc., Eugene, OR) was added; the mixture was incubated at 37 °C with shaking. After 1 h, phase separation was performed, and the aqueous supernatant was recovered. Buffer and enzyme were added again, and the procedure was repeated. The two resulting supernatants were pooled, and the proteins were recovered by acetone precipitation, separated by SDS-PAGE, and visualized by silver staining. Protein bands were cut out and in-gel digested with trypsin (34).

Western Blot Analysis—The GPI-enriched fraction was separated by SDS-PAGE and transferred to polyvinylidene difluoride membranes. Immunoblotting against cross-reacting determinant (CRD) was performed as described previously (35–37).

Mass Spectrometry—Automated nanoflow liquid chromatography-tandem mass spectrometric analysis was performed using a quadrupole time-of-flight Ultima mass spectrometer (Micromass UK Ltd., Manchester, UK) employing automated data-dependent acquisition. A nanoflow HPLC system (UltiMate, Switchos2, FAMOS from LC Packings, Amsterdam, The Netherlands) was used to deliver a flow rate of 175 nl/min. Chromatographic separation was accomplished by loading peptide samples onto a homemade 2-cm fused silica precolumn (75-μm inner diameter and 360-μm outer diameter; Zorbax® SB-C18 5 μm, Agilent, Wilmington, DE) using autosampler essentially as described by Licklider *et al.* (38). Sequential elution of peptides was accomplished using a linear gradient from Solution A (0% acetonitrile in 1% formic acid, 0.6% acetic acid, 0.005% heptafluorobutyric acid) to 40% of Solution B (90% acetonitrile in 1% formic acid, 0.6% acetic acid, 0.005% heptafluorobutyric acid) in 30 min over the precolumn in-line with a homemade 8-cm resolving column (75-μm inner diameter and 360-μm outer diameter; Agilent Zorbax® SB-C18 3.5 μm). The resolving column was connected using a fused silica transfer line (20-μm inner diameter) to a distally coated fused silica emitter (360-μm outer diameter, 20-μm inner diameter, 10-μm tip inner diameter; New Objective, Cambridge, MA) biased to 2.6 kV.

The mass spectrometer was operated in the positive ion electrospray ionization mode with a resolution of 9,000–11,000 full-width half-maximum using a source temperature of 80 °C and a countercurrent nitrogen flow rate of 150 liters/h. Data-dependent analysis was employed (three most abundant ions in each cycle): 1-s mass spectrometry (*m/z* 350–1,500) and maximum 4-s MS/MS (*m/z* 50–2,000, continuum mode) with 30-s dynamic exclusion. A charge state recognition algorithm was employed to determine optimal collision energy for low energy collision-induced dissociation MS/MS of peptide ions. External mass calibration using NaI resulted in mass errors of less than 50 ppm, typically 5–15 ppm in the *m/z* range 50–2,000. Raw data was processed using MassLynx 3.5 ProteinLynx (smooth 3/2 Savitzky Golay and center 4 channels/80% centroid), and the resulting MS/MS dataset was exported in the Micromass pkl format. Automated peptide identification from raw data was performed using an in-house MASCOT server (version 1.8) (Matrix Sciences, London, UK) using the National Center for Biotechnology Information (NCBI) non-redundant protein database with the following constraints: tryptic cleavage after Arg and Lys, up to two missed cleavage sites, and tolerance of ±0.5 for MS and ±0.2 for MS/MS fragment ions. Carbamidomethylcysteine (C) was specified as a fixed modification, and deamidation of Asn and Gln and oxidation of Met were specified as partial modifications. Most of the GPI-APs (five of six in HeLa cells and 34 of 44 in *A. thaliana* cells) were identified based on two or more different peptide tandem mass spectra matching to each individual protein. A total of 11 GPI-APs were each identified based on one peptide sequence obtained by tandem mass spectrometry (one in HeLa cells and 10 in *A. thaliana* cells). In these cases the tandem mass spectra were manually inspected to validate the data and the corresponding protein sequence assignments.

RESULTS

Selective Isolation of GPI-anchored Proteins

We have integrated protein fractionation methods, mass spectrometry, and bioinformatics techniques into a proteomic

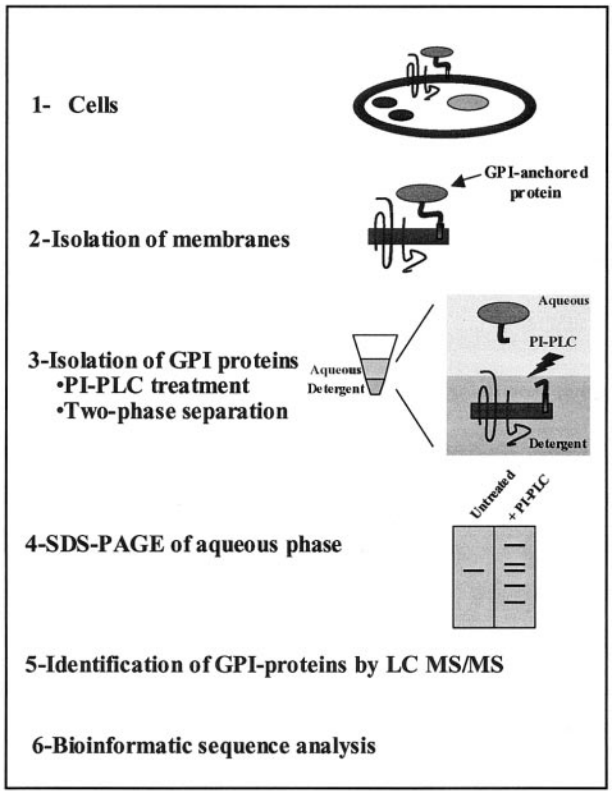

FIG. 1. **Modification-specific proteomic strategy for isolation and identification of GPI-anchored proteins by mass spectrometry.** *LC*, liquid chromatography.

"shave-and-conquer" strategy aimed at defining an extensive inventory of GPI-APs in human and plant cells. The strategy is summarized in Fig. 1. Triton X-114 detergent-based two-phase separation was used for partitioning membrane proteins and soluble proteins (33) in membrane fractions from *Homo sapiens* (raft-enriched fractions) and *A. thaliana* (microsomes). The isolated membrane fractions were treated with phosphatidylinositol phospholipase C (*Bacillus cereus,* PI-PLC) enzyme in the presence of Triton X-114 by adapting the method of Hooper *et al.* (39). This enzyme hydrolyzes the phosphatidylinositol, releasing the soluble GPI protein from the membrane/detergent phase and enabling its recovery in the aqueous phase. As the PI-PLC enzyme used in the present study recognizes a specific GPI anchor structure, probably only a subset of GPI-APs is released from the membrane preparations. Some GPI anchors are modified by acylation at the 2- and/or 3-position of the inositol ring prohibiting cleavage by PI-PLC (40).

The protein sample isolated in this way was concentrated by precipitation and separated by SDS-PAGE. Silver staining of the SDS-PAGE gels demonstrated that a range of proteins were selectively recovered upon PI-PLC treatment of human raft-enriched membranes (Fig. 2*A*, *II*) and plant membrane preparations (Fig. 2*B*, *IV*) as compared with the untreated samples. Furthermore, Western blotting using anti-CRD antibody specific for the C terminus of PI-PLC-treated GPI-anchored protein demonstrated that GPI-APs were highly enriched in the aqueous phase after PI-PLC treatment of raft-enriched membranes (Fig. 2*A*, *I*) and plant membranes (Fig. 2*B*, *III*). In summary, these data demonstrate that membrane fractionation methods in combination with PI-PLC treatment enable significant enrichment of a range of GPI-anchored proteins from human and plant cells.

Protein Identification by Tandem Mass Spectrometry and Bioinformatics

Identification of GPI-APs in Human Lipid Raft-enriched Fractions—Next, the recovered proteins were analyzed and identified by mass spectrometry. Twelve consecutive protein bands were excised from the SDS-PAGE gel containing the GPI-AP-enriched fraction from human raft-enriched fractions as indicated in Fig. 2*A*. Protein samples were in-gel digested with trypsin, and the recovered peptides were separated and sequenced by nanoscale HPLC interfaced to electrospray ionization quadrupole time-of-flight tandem mass spectrometry. For each nanoscale liquid chromatography-MS/MS run, the complete set of peptide tandem mass spectra was submitted for protein sequence database searching. A total of 17 human proteins were identified (Table I) comprising the initial set of putative GPI-APs. To eliminate false positive and false negative assignments of GPI-APs among this set of proteins we applied computational methods for amino acid sequence analysis and assignments of GPI-APs.

Two GPI-AP prediction tools, big-PI (mendel.imp.univie.ac.at/gpi/gpi_server.html) and DGPI (www.expasy.org/tools/), were used to screen the 17 candidate human GPI-APs. Six known human GPI-APs were correctly assigned by both methods, except carboxypeptidase M, which was not predicted by big-PI (Table I). In addition, the 11 identified proteins that are not members of the GPI-anchored protein family were also correctly assigned as such by these computational methods (Table I). This lack of false positive assignments is in accordance with a recent report that estimates the sensitivity of current GPI-AP prediction tools to be 80–90% with a false positive rate of only 0.1–0.2% (41).

Thus, the combination of sensitive, selective, and specific experimental and computational proteomic methods facilitates identification and assignment of GPI-anchored membrane proteins. This is further illustrated by the fact that these six human GPI-APs comprise the largest set of GPI-APs recovered and identified in a single study of lipid raft-enriched membranes to date.

Identification of GPI-APs from A. thaliana Cell Membranes—The general utility of the integrated experimental and computational strategy for identification of GPI-APs was investigated by using an *A. thaliana* cell membrane preparation (see "Experimental Procedures"). PI-PLC treatment and SDS-PAGE separation demonstrated significant enrichment of

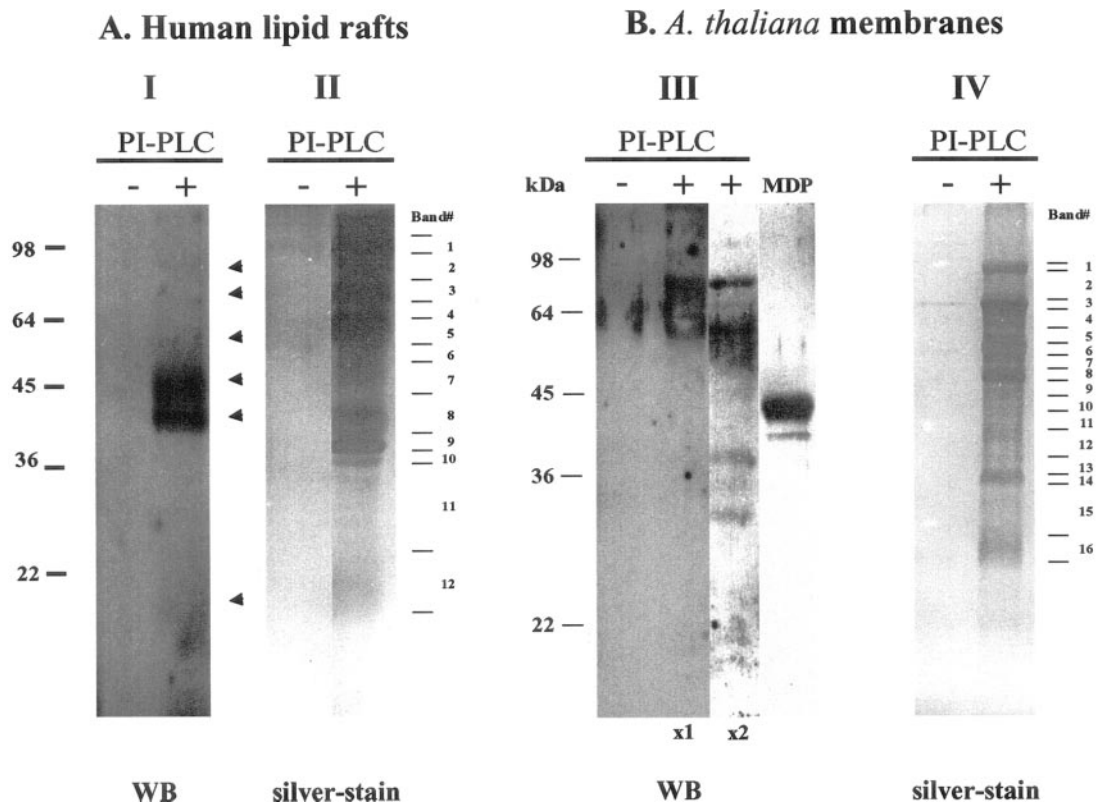

FIG. 2. **Isolation and detection of GPI-APs from human and plant cells.** Treatment with PI-PLC and two-phase separation by detergent followed by SDS-PAGE separation of the recovered proteins provide a differential display readout of GPI-anchored proteins. *A*, human lipid raft-enriched membranes. *I*, Western blotting (*WB*) against CRD antibody of the aqueous fractions after two-phase separation, with and without PI-PLC treatment of the HeLa raft-enriched fraction. Recognized GPI-APs are marked by a *small arrow*. *II*, 12% SDS-PAGE of the aqueous fractions after two-phase separation, with and without PI-PLC treatment of raft-enriched membranes. *Band#*, excised bands. *B*, *A. thaliana* membrane preparation. *III*, Western blotting against CRD antibody of aqueous fractions after two-phase separation, with and without PI-PLC treatment of *A. thaliana* enriched plasma membranes. *×1* and *×2* refer to the protein load on the gel. *MDP*, pig membrane dipeptidase as a positive control for CRD antibody. *IV*, 12% SDS-PAGE of the aqueous fractions after two-phase separation, with and without PI-PLC treatment of *A. thaliana* plasma membranes.

GPI-anchored proteins (Fig. 2*B*). A total of 16 protein bands (Fig. 2*B*, *IV*) were cut out, processed, and analyzed by mass spectrometry. The liquid chromatography-MS/MS data obtained from Band 1 is shown in Fig. 3. The tandem mass spectrum corresponding to the tryptic peptide VDDGDSEISLDR was the only detectable peptide originating from the At4g27520 protein in this experiment. Nevertheless, the high quality of the quadrupole time-of-flight tandem mass spectrum enabled unambiguous identification of the cognate protein via protein sequence database searching. A total of seven proteins were identified in Band 1. Overall, sequence database searching by peptide tandem mass spectra led to the identification of a total of 64 proteins in the 16 protein bands obtained from the SDS-PAGE gel (Tables II and III).

Because of the lack of general and sensitive techniques for experimental verification of the 64 putative GPI-APs identified in this experiment, we again applied bioinformatics methods to further characterize these proteins. In addition to big-PI and DGPI, the list of putative *A. thaliana* GPI-APs predicted by Dupree and co-workers (18) (mips.gsf.de/proj/thal/db/index.html) was reviewed.

Of the 64 identified proteins, 44 were predicted to be GPI-APs by at least one of the computational techniques (Table I). Sixteen of the identified proteins were assigned as GPI-APs by two of the three computational methods, whereas 26 proteins were assigned as GPI-APs by all three methods. Two β-1,3-glucanases were assigned as GPI-APs by one computational method only: At2g27500 as predicted by DGPI and At5g61130 as predicted by Borner *et al.* (18). None of the three computational techniques assigned all of the 44 GPI-APs, suggesting that further tuning is necessary and that the combination of several experimental and computational techniques is advantageous for this purpose.

The 20 "contaminant proteins" were all assigned as non-GPI-APs by all three computational methods (Table III). They either correspond to secreted proteins (*i.e.* had only a signal peptide but no hydrophobic C terminus) or were regular mem-

TABLE I

Proteins identified by modification-specific proteomic analysis for determination of GPI-anchored proteins in human lipid raft-enriched membranes

Swiss Prot, Swiss-Prot accession number. B, protein band number on SDS-PAGE gel. #, number of unique peptides matched for each protein. Score, score obtained in MASCOT database search (significance threshold of 54). big-PI, mendel.imp.univie.ac.at/gpi/gpi_server.html. DGPI, 129.194.185.165/dgpi/index_en.html. A filled circle means that the protein has been recognized as a GPI-AP, and an open circle means that the protein has not been recognized as a GPI-AP.

Protein identification					GPI-AP prediction	
Swiss Prot	B	Name	#	Score	DGPI	big-PI
GPI-anchored proteins						
P05186	3	Alkaline phosphatase	11	322	●	●
P14384	4	Carboxypeptidase M	2	79	●	○
P08174	5	Decay acceleration factor, CD55	9	376	●	●
Q03405	6	Urokinase plasminogen activator receptor (UPAR)	1	62	●	●
P15328	8	Folate receptor 1	8	279	●	●
P13987	12	CD59 glycoprotein	3	131	●	●
Proteins						
P21796	1	Voltage-dependent anion channel	4	191	○	○
P05556	1	Fibronectin receptor, CD29	13	585	○	○
P43121	2	Melanoma adhesion molecule, CD146	2	80	○	○
P16070	3	Epican, CD44	2	75	○	○
P08195	3	4F2 heavy chain antigen, CD98	4	181	○	○
P11021	3	78-kDa glucose-regulated protein	15	768	○	○
Q9UK57	6	Mesotheline/megakaryocyte potentiation factor	3	91	○	○
P15999	9	ATP synthase α chain	3	159	○	○
Q9NZS6	9	Glucocorticoid receptor AF-1-specific elongation factor	3	104	○	○
P02571/P02572	9	Actin, β and/or γ actin	4	147	○	○
P11912	10	B-cell antigen receptor complex-associated protein α chain, CD79	3	135	○	○

brane proteins (*i.e.* contained at least one "true" transmembrane domain).

We manually inspected the 44 positively assigned GPI-anchored protein sequences and found that all of them had a cleavable signal peptide, a hydrophobic C terminus of at least 10 residues, and no internal transmembrane domains, as found by "Membrane Protein Explorer" (blanco.biomol.uci.edu/mpex/). We could assign putative ω-sites to most of the 44 GPI-APs (Fig. 4), which represented Ser, Ala, Asn, or Gly residues and were 8–11 residues upstream of the hydrophobic C terminus. In some cases, up to two large residues were found near the ω-site. These observations suggest an unusually large flexibility in the length of the spacer region as well as volume compensation in the active site that recognizes the $\omega - 1$–$\omega + 2$ site (14).

DISCUSSION

Systematic functional analysis of large sets of proteins is a bottleneck in proteomic studies. Integration of experimental and computational tools is therefore a prerequisite for recovering the wealth of information available in proteomic datasets. We have demonstrated the feasibility of integrating biochemical, mass spectrometry, and computational techniques for selective, specific, and sensitive identification of GPI-anchored membrane proteins. This targeted modification-specific proteomic strategy was initially applied to the analysis of GPI-APs in a raft-enriched membrane preparation from human HeLa cells. Of 17 recovered proteins, six were shown to be *bona fide* GPI-APs. This total is the largest number of GPI-APs recovered and identified in a single experimental study of lipid raft-enriched membranes, and, reassuringly, five of the six proteins identified are known from other studies to reside in lipid rafts. In addition, this is the first indication that urokinase plasminogen activator receptor may be localized in lipid rafts.

A recent proteomic investigation of HeLa lipid rafts resulted in the identification of five GPI-APs (folate receptor, alkaline phosphatase, CD55, 5′-nucleotidase, and Kilon) among 241 authentic lipid raft components (11). These GPI-APs were each identified based on one peptide tandem mass spectrum except alkaline phosphatase (five peptides). In contrast, the present strategy demonstrates that GPI-APs can be selectively enriched, identified, and assigned in a targeted shave-and-conquer approach as illustrated by the fact that six GPI-APs were determined in a set of only 17 proteins. These six proteins were identified based on up to 11 peptides (Table I), suggesting that it may in some cases be feasible to recover and detect the elusive C-terminal peptides, which contain the remainder of the GPI anchors. Current studies in our laboratory are focused on this issue.

GPI anchoring of cell surface proteins is likely to play an important role in plants as in other eukaryotes, but experimental data on their expression and distribution have been scarce so far. We chose this poorly characterized yet physiologically and developmentally extremely important "subproteome" of the model plant *Arabidopsis* to demonstrate the scope of modification-specific proteomics.

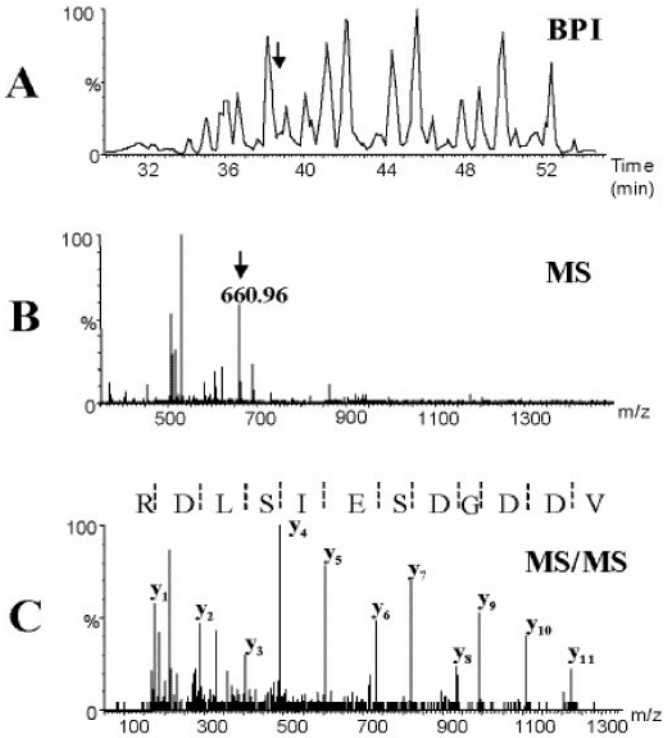

FIG. 3. **Mass spectrometry analysis.** *A*, base peak ion chromatogram (*BPI*) of tryptic peptides obtained by nanoscale liquid chromatography-MS/MS analysis of Band 1 in Fig. 2*B*, *IV*. *B*, mass spectrum obtained from the eluting peptides at time 38.65 min. *C*, MS/MS spectrum of the peptide ion marked in *panel B* and the amino acid sequence obtained. This sequence identified At4g27520 (phytocyanin-like) protein with a MASCOT score of 104 (significance threshold of 54). Note that the N terminus of the peptide is on the *right* and the C terminus is on the *left*.

Among the 44 validated GPI-APs, 34 proteins were identified based on two or more peptide tandem mass spectra matching to each individual protein sequence. The highest sequence coverage was obtained for the SKU5 protein and the glycerophosphodiesterases, indicating that these proteins are the most abundant in the preparation. A total of 10 GPI-APs were each identified based on one peptide sequence obtained by tandem mass spectrometry. In these cases the tandem mass spectra were manually inspected to validate the data and the corresponding protein sequence assignments. The 44 validated GPI-APs were on average identified on the basis of 4.5 individual peptides, whereas the 20 contaminant proteins were, on average, identified by less than two peptides, except the reticuline oxidase-like protein, suggesting a strong enrichment of GPI-APs in the protein preparation (Table II). Ultimately, proteins were assigned "contaminants" solely on the basis of predicted topology. The "leaking" of the aquaporins with six transmembrane domains into the aqueous phase was unexpected. In summary a total of 44 GPI-APs were determined in a population of 64 identified proteins, illustrating the high specificity of the experimental and computational proteomic strategy.

As would be expected for *bona fide* GPI-APs none of the 44 proteins produced tryptic peptide signals originating from amino acid sequences located beyond the ω-sites, supporting the assumption that these GPI-APs were C-terminally processed prior to addition of the GPI anchor. In no case were we able to identify the definitive signal of a C-terminal peptide carrying the portion of the GPI anchor that remains after PI-PLC treatment. We expect such C-terminal "glycopeptides" to be very hydrophilic and difficult to ionize and to fragment inefficiently in tandem mass spectrometry experiments. We are currently exploring mass spectrometry-based approaches (42) to detect and characterize these species at subpicomole levels.

Many of the identified GPI-APs are rare transcripts, judged by Massively Parallel Signature Sequencing (MPSS) database expression analysis of *Arabidopsis* callus tissue (mpss.ucdavis.edu/java.html), and frequently no expressed sequence tags of these genes have been published (mips.gsf.de/proj/thal/db/index.html) (MPSS and ESTs columns in Table II), as in the case of the protease encoded by At5g10080. These data suggest that our approach has a very wide dynamic range and covers both highly abundant and rare proteins. Interestingly, however, the abundance of some protein in our preparation (as estimated by the number of peptides) shows little correlation with the expression data; the glycerophosphodiesterase-like protein encoded by At4g26690 was identified with 17 peptides but was not found by MPSS in callus tissue.

Only a proteomic approach can give in-depth information on GPI-APs in *Arabidopsis* because the prediction of this modification from gene sequences is not fully reliable and because existing prediction tools rely to a certain extent on experimental input from unrelated organisms. A recent two-dimensional electrophoresis-based proteomic study (18) led to fine tuning of the sequence analysis algorithm, thereby providing a more comprehensive and accurate prediction of the *Arabidopsis* GPI-anchored proteome.

The 44 GPI-APs determined in the present study constitute ~18% of the predicted GPI-anchored proteome of *A. thaliana* and represent virtually all predicted protein families (18). We provide the first biochemical evidence of GPI anchoring for the protease and polygalacturonase families. In addition to previously known or predicted protein families, we identified a truncated phospholipase C-like protein containing only the PLC-X domain (At5g67130). This protein and At2g27500 were not predicted as GPI-APs by the computational method of Borner *et al.* (18); however, they were assigned as GPI-APs by DGPI or big-PI (Table II). This type of information is valuable for further tuning and optimization of the computational GPI-AP predictors as well as for design of experimental studies for functional analysis.

A large number of the identified GPI-anchored proteins is involved in cell wall remodeling, among them multiple putative β-1,3-glucanases, a polygalacturonidase, and the BP 10-like

TABLE II

GPI-APs identified by modification-specific proteomic analysis of A. thaliana plasma membranes

AGI, *Arabidopsis* Genome Initiative code. B, protein band number on SDS-PAGE gel. #, number of unique peptides matched for each protein/protein family. Score, score obtained in MASCOT database search (significance threshold of 54). MPSS, comparison of estimated protein levels and available expression data. Quantitative expression data for the genes in callus tissue (in ppm) have been obtained by Massive Parallel Signature Sequencing (MPSS, mpss.ucdavis.edu/java.html) where/means no data available. ESTs, expressed sequence tags. The number of published ESTs corresponding to the genes has been obtained from the Munich *A. thaliana* database (MATDB, mips.gsf.de/proj/thal/db/index.html). DGPI (www.expasy.org/tools), big-PI (mendel.imp.univie.ac.at/gpi/gpi_server.html), and Borner *et al.*: Proteins were recognized as GPI-APs after searching with these predictors and after reviewing the list of *A. thaliana* GPI-APs predicted by Dupree and co-workers (mips.gsf.de/proj/thal/db/index.html). A filled circle means that a protein has been recognized as a GPI-AP, and an open circle means that a protein has not been recognized as GPI-AP.

Protein identification							GPI-AP prediction		
AGI code	B	Protein family	#	Score	MPSS	ESTs	DGPI	big-PI	Borner *et al.* (Ref. 18)
At1g32860	9	β-1,3-glucanase	2	57	/	2	●	●	●
At1g64760	6	β-1,3-glucanase	11	300	30	0	○	●	●
At2g27500	11	β-1,3-glucanase	3	123	8	9	●	○	○
At3g13560	4	β-1,3-glucanase	2	94	/	3	●	●	●
At4g29360	4	β-1,3-glucanase	1	39	/	1	●	●	●
At4g31140	8	β-1,3-glucanase	15	533	108	3	●	●	●
At5g08000	16	β-1,3-glucanase	3	73	0	6	●	●	●
At5g42100	9	β-1,3-glucanase	3	63	45	17	●	●	●
At5g56590	5	β-1,3-glucanase	2	106	13	5	●	○	●
At5g58480	5	β-1,3-glucanase	8	375	/	3	●	●	●
At5g61130	16	β-1,3-glucanase	2	66	140	2	○	○	●
At2g01630	4	β-1,3-glucanase and EGF-like domain	8	327	0	5	●	●	●
At4g25240	4	BP10-like, pectinesterase family	11	472	21	1	●	○	●
At4g12420	3	BP10-like/SKU5	18	879	/	12	●	●	●
At5g51480	7	BP10-like/SKU5	4	193	1	3	●	●	●
At3g29810	5	COBRA	1	62	/	0	●	●	●
At4g16120	2	COBRA	3	106	/	4	●	○	●
At5g67130	10	Contains PLC-X domain	7	354	40	5	●	●	○
At3g07390	2	DoH domain	5	174	60	13	○	●	●
At2g45470	2	Fasciclin-like	7	355	15	38	●	○	●
At3g60900	5	Fasciclin-like	2	99	12	4	●	○	●
At5g55730	4	Fasciclin-like	1	64	0	11	●	●	●
At5g44130	7	Fasciclin-like	11	417	0	4	●	●	●
At2g04780	3	Fasciclin-like AGP	3	64	28	27	●	●	●
At4g12730	13	Fasciclin-like AGP-2	3	117	5	40	●	○	●
At3g46550	5	Fasciclin-like SOS5	1	36	16	1	●	○	●
At4g26690	1	Glycerophosphodiesterase-like	17	698	0	15	●	●	●
At5g55480	1	Glycerophosphodiesterase-like	14	707	0	9	●	●	●
At5g58090	7	Glycerophosphodiesterase-like	1	60	100	9	●	●	●
At1g74790	5	Hedgehog-interacting protein (HIP)-like	4	111	49	5	○	●	●
At2g13820	2	Lipid-transfer protein-like (LTPL)	2	71	/	8	●	○	●
At2g27130	9	Lipid-transfer protein-like (LTPL)	1	36	6	0	●	●	●
At5g64080	1	Lipid-transfer protein-like (LTPL)	1	43	34	7	●	●	●
At4g27520	1	Phytocyanin-like (early nodulin-like)	1	104	129	25	●	●	●
At5g25090	1	Phytocyanin-like (early nodulin-like)	2	104	14	0	●	●	●
At5g20230	15	Phytocyanin-like (stellacyanin-like)	2	41	156	8	●	●	●
At5g15350	15	Plastocyanin-like domain	1	30	305	15	●	○	●
At3g15720	9	Polygalacturonase	4	150	44	0	○	●	●
At5g10080	5	Protease	2	70	0	0	●	○	●
At1g77630	1	Receptor-like kinase	2	80	8	7	●	●	●
At2g17120	8	Receptor-like kinase	7	273	1	19	●	●	●
At1g61900	4	Unknown	2	63	43	9	●	●	●
At4g28100	9	Unknown	2	92	/	4	●	●	●
At5g19250	14	Unknown	1	51	0	15	●	○	●

proteins, putative pectin methylesterases. The large number of GPI-anchored glucanases was unexpected and hints at a surprising functional diversity of these proteins. None of them co-clustered with well characterized pathogenesis-related proteins by primary structure or expression pattern (The *Arabidopsis* Information Resource (TAIR) database, www.arabidopsis.org/tools/bulk/microarray/index.html; data not shown). β-1,3-Glucanases have a known role, apart from pathogen defense, in the regulation of plasmodesmata size (43) and seed ripening (44), and the various identified GPI-anchored enzymes may have unanticipated roles in remodeling of the endogenous plant β-1,3-glucan, callose. A second

TABLE III
Non-GPI-APs from A. thaliana

AGI, *Arabidopsis* Genome Initiative code. B, protein band number on SDS-PAGE gel. #, number of unique peptides matched for each protein/protein family. Score, score obtained in MASCOT database search (significance threshold of 54). TM, number of transmembrane domains predicted for the protein. DGPI (www.expasy.org/tools/), big-PI (mendel.imp.univie.ac.at/gpi/gpi_server.html), and Borner *et al.*: Proteins were recognized as GPI-APs after searching these predictors and after reviewing the list of *A. thaliana* GPI-APs predicted by Dupree and co-workers (mips.gsf.de/proj/thal/db/index.html). A filled circle means that the protein has been recognized as a GPI-AP, and an open circle means that the protein has not been recognized as a GPI-AP.

Protein identification						GPI-AP prediction		
AGI code	B	#	TM	Notes	Score	DGPI	big-PI	Borner *et al.*
At3g46900	11	1	3	Copper transporter, COPT2	61	○	○	○
At3g25290	11	1	1	DoH and cytochrome b_{561} domains	44	○	○	○
At5g35735	12	2	5	DoH and cytochrome b_{561} domains	99	○	○	○
At2g16850	11	1	6	PIP	42	○	○	○
At3g61430	16	3	6	PIP1a	120	○	○	○
At2g45960	9	1	6	PIP1b	96	○	○	○
At4g35100	9	1	6	PIP3	54	○	○	○
At4g20830	6	25	0	Reticuline oxidase-like-secreted	1281	○	○	○
At3g02880	1	1	1	Receptor-like kinase	41	○	○	○
At3g17840	10	2	1	Receptor-like kinase	49	○	○	○
At1g53840	13	1	0	Secreted	69	○	○	○
At5g46700	16	1	4	Senescence-associated protein	32	○	○	○
At3g44150	14	1	0	Unknown, secreted	29	○	○	○
At3g11820	13	2	1	Syntaxin 121	59	○	○	○
At5g08080	13	2	1	Syntaxin 132	80	○	○	○
At3g09740	15	3	1	Syntaxin 71	101	○	○	○
At3g54200	13	2	1	Transmembrane (TM)	67	○	○	○
At5g11890	11	1	1	TM	28	○	○	○
At2g12400	4	1	3–6	TM	56	○	○	○
At3g17350	11	3	0	Unknown, secreted	92	○	○	○

large family of GPI-APs were proteins with fasciclin-like domains. The domain is conserved in all eukaryotes (45) and has putative signaling roles in cell adhesion. Because of the chemically very different nature of the plant and animal extracellular matrix, this conservation among eukaryotes is surprising, and more biochemical studies need to address the role of the plant cell wall in signaling (46).

Conspicuously, no representative of the "classical" arabinogalactan proteins (17, 18) is among the identified GPI-APs. It is possible that they are not expressed to a high level in the dedifferentiated cell culture, that the extensive glycosylation prevents tryptic cleavage, or that they have largely been "shed" from the membrane by intrinsic phospholipase activity (47) and thus have been lost in the TX-114 partitioning. Many of the other proteins, however, contain possible arabinogalactan modification motifs. Two proteins, SKU5 and SOS5, have a demonstrated role in cell expansion (22, 23), probably also the two members of the COBRA family (15). It is thus possible to identify key regulators of growth and development, some of them proteins of low abundance, in a targeted proteomic strategy. Although the plant-specific prediction tool identified almost the complete set of GPI-APs found in the experimental dataset, the other two predictors together would lead to the same conclusion, only lacking the At5g61130 β-1,3-glucanase but rescuing the already mentioned At2g27500 and At5g67130, emphasizing the need for complementary computational and experimental methods in proteomics research projects. Post-translational modifications are predicted from gene sequences with various degrees of accuracy, and there is a great need for development of sensitive and robust mass spectrometry-based techniques for their determination (29, 48). In all cases the experimental studies at the protein level result in unambiguous assignments of post-translational modifications and will in turn lead to better design of post-translational modification prediction tools. A similar note of caution is valid for protein levels; we have found substantial discrepancy between estimated protein abundance (by the number of identifying peptides) and MPSS expression data in callus, a tissue very similar to the suspension culture.

In conclusion we have reported the largest number of experimentally determined GPI-APs to date. The modification-specific proteomic strategy presented here for human and plant samples should be applicable to the study of GPI-anchored membrane proteins in a variety of eukaryotic cell types. The diagnostic and therapeutic potential of cell surface proteins in medicine has been widely appreciated. Similarly, the identification of GPI-APs in plants could aid the development of enhanced and novel approaches to identification of agrochemicals that can regulate intracellular responses without having to cross cell membranes. Mutants in three GPI-APs were found to have severe abnormalities in root development. The ability to use herbicides that would target such proteins would offer several safety advantages over many of

FIG. 4. **Localization of the ω-sites in GPI-APs.** Shown is the alignment of C termini of the GPI-APs. Hydrophobic amino acids of the C terminus are marked in *gray*, and potential ω-sites are *underlined*. If the ω-site appears unambiguous, it is marked in *bold type*. In some cases, up to two large residues were found near the ω-site. These observations suggest an unusually large flexibility in the length of the spacer region as well as volume compensation in the active site that recognizes the $\omega - 1$–$\omega + 2$ site (14).

the current agrochemicals. Because these chemicals would not need to permeate membranes, they would be unlikely to have effects on users or on non-target organisms. Consequently the use of such chemicals would have benefits for farm workers and for the environment.

Acknowledgments—CRD antibody was kindly provided by Professor N. M. Hooper of University of Leeds. Dr. J. Bunkenborg is acknowledged for helpful discussions.

* This work was supported by a grant from the Danish Natural Sciences Research Council (to O. N. J.) and by funds from the Gatsby Charitable Foundation (to T. S. N. and S. C. P.). The costs of publication of this article were defrayed in part by the payment of page charges. This article must therefore be hereby marked "*advertisement*" in accordance with 18 U.S.C. Section 1734 solely to indicate this fact.

§ Supported by a post-doctoral fellowship from the Basque Government.

‖ Supported by a European Molecular Biology Organization short term fellowship.

** Supported by a European Molecular Biology Organization long term fellowship.

‡‡ To whom correspondence should be addressed. Tel.: 45-6550-2368; Fax: 45-6550-2467; E-mail: jenseno@bmb.sdu.dk.

REFERENCES

1. Ferguson, M. A., Homans, S. W., Dwek, R. A., and Rademacher, T. W. (1988) Glycosyl-phosphatidylinositol moiety that anchors Trypanosoma brucei variant surface glycoprotein to the membrane. *Science* 239, 753–759
2. Hooper, N. M. (1997) Glycosyl-phosphatidylinositol anchored membrane enzymes. *Clin. Chim. Acta* **266,** 3–12
3. Ferguson, M. A. (1999) The structure, biosynthesis and functions of glycosylphosphatidylinositol anchors, and the contributions of trypanosome research. *J. Cell Sci.* **112,** 2799–2809
4. Angst, B. D., Marcozzi, C., and Magee, A. I. (2001) The cadherin superfamily: diversity in form and function. *J. Cell Sci.* **114,** 629–641
5. Ghiran, I., Klickstein, L. B., and Nicholson-Weller, A. (2003) Calreticulin is at the surface of circulating neutrophils and uses CD59 as an adaptor molecule. *J. Biol. Chem.* **278,** 21024–21031
6. Horejsi, V., Drbal, K., Cebecauer, M., Cerny, J., Brdicka, T., Angelisova, P., and Stockinger, H. (1999) GPI-microdomains: a role in signalling via immunoreceptors. *Immunol. Today* **20,** 356–361
7. Muniz, M., and Riezman, H. (2000) Intracellular transport of GPI-anchored proteins. *EMBO J.* **19,** 10–15
8. Nishizuka, Y. (1995) Protein kinase C and lipid signaling for sustained cellular responses. *FASEB J.* **9,** 484–496
9. Harder, T., Scheiffele, P., Verkade, P., and Simons, K. (1998) Lipid domain structure of the plasma membrane revealed by patching of membrane components. *J. Cell Biol.* **141,** 929–942
10. Peskan, T., Westermann, M., and Oelmuller, R. (2000) Identification of low-density Triton X-100-insoluble plasma membrane microdomains in higher plants. *Eur. J. Biochem.* **267,** 6989–6995
11. Foster, L. J., De Hoog, C. L., and Mann, M. (2003) Unbiased quantitative proteomics of lipid rafts reveals high specificity for signaling factors. *Proc. Natl. Acad. Sci. U. S. A.* **100,** 5813–5818
12. Hooper, N. M. (2001) Determination of glycosyl-phosphatidylinositol membrane protein anchorage. *Proteomics* **1,** 748–755
13. Udenfriend, S., and Kodukula, K. (1995) How glycosylphosphatidylinositol-anchored membrane proteins are made. *Annu. Rev. Biochem.* **64,** 563–591
14. Eisenhaber, B., Bork, P., and Eisenhaber, F. (1998) Sequence properties of GPI-anchored proteins near the omega-site: constraints for the polypeptide binding site of the putative transamidase. *Protein Eng.* **11,** 1155–1161
15. Roudier, F., Schindelman, G., DeSalle, R., and Benfey, P. N. (2002) The COBRA family of putative GPI-anchored proteins in Arabidopsis. A new fellowship in expansion. *Plant Physiol.* **130,** 538–548
16. Eisenhaber, B., Bork, P., and Eisenhaber, F. (2001) Post-translational GPI lipid anchor modification of proteins in kingdoms of life: analysis of protein sequence data from complete genomes. *Protein Eng.* **14,** 17–25
17. Borner, G. H., Sherrier, D. J., Stevens, T. J., Arkin, I. T., and Dupree, P. (2002) Prediction of glycosylphosphatidylinositol-anchored proteins in Arabidopsis. A genomic analysis. *Plant Physiol.* **129,** 486–499
18. Borner, G. H., Lilley, K. S., Stevens, T. J., and Dupree, P. (2003) Identification of glycosylphosphatidylinositol-anchored proteins in Arabidopsis. A proteomic and genomic analysis. *Plant Physiol.* **132,** 568–577
19. Takos, A. M., Dry, I. B., and Soole, K. L. (2000) Glycosyl-phosphatidylinositol-anchor addition signals are processed in Nicotiana tabacum. *Plant J.* **21,** 43–52
20. Oxley, D., and Bacic, A. (1999) Structure of the glycosylphosphatidylinositol anchor of an arabinogalactan protein from Pyrus communis suspension-cultured cells. *Proc. Natl. Acad. Sci. U. S. A.* **96,** 14246–14251

21. Schindelman, G., Morikami, A., Jung, J., Baskin, T. I., Carpita, N. C., Derbyshire, P., McCann, M. C., and Benfey, P. N. (2001) COBRA encodes a putative GPI-anchored protein, which is polarly localized and necessary for oriented cell expansion in Arabidopsis. *Genes Dev.* **15,** 1115–1127
22. Sedbrook, J. C., Carroll, K. L., Hung, K. F., Masson, P. H., and Somerville, C. R. (2002) The Arabidopsis SKU5 gene encodes an extracellular glycosyl phosphatidylinositol-anchored glycoprotein involved in directional root growth. *Plant Cell* **14,** 1635–1648
23. Shi, H., Kim, Y., Guo, Y., Stevenson, B., and Zhu, J. K. (2003) The Arabidopsis SOS5 locus encodes a putative cell surface adhesion protein and is required for normal cell expansion. *Plant Cell* **15,** 19–32
24. Takos, A. M., Dry, I. B., and Soole, K. L. (1997) Detection of glycosylphosphatidylinositol-anchored proteins on the surface of Nicotiana tabacum protoplasts. *FEBS Lett.* **405,** 1–4
25. Sherrier, D. J., Prime, T. A., and Dupree, P. (1999) Glycosylphosphatidylinositol-anchored cell-surface proteins from Arabidopsis. *Electrophoresis* **20,** 2027–2035
26. Fivaz, M., Vilbois, F., Pasquali, C., and van der Goot, F. G. (2000) Analysis of glycosyl phosphatidylinositol-anchored proteins by two-dimensional gel electrophoresis. *Electrophoresis* **21,** 3351–3356
27. Elortza, F., Foster, L. J., Stensballe, A., Zeemann, P., and Jensen, O. N. (2002) *Presentations of the 14th Meeting Methods of Protein Structure Analysis, Valencia, September 8–12, 2002*, p. 89, International Association Protein Structure Analysis and Proteomics, Charlottesville, VA
28. Jensen, O. N. (2000) in *Proteomics: A Trends Guide* (Blackstock, W., and Mann, M., eds) pp. 36–42, Elsevier Science Publishing Co., Inc., New York
29. Mann, M., and Jensen, O. N. (2003) Proteomic analysis of post-translational modifications. *Nat. Biotechnol.* **21,** 255–261
30. Smart, E. J., Ying, Y. S., Mineo, C., and Anderson, R. G. (1995) A detergent-free method for purifying caveolae membrane from tissue culture cells. *Proc. Natl. Acad. Sci. U. S. A.* **92,** 10104–10108
31. Nuhse, T. S., Peck, S. C., Hirt, H., and Boller, T. (2000) Microbial elicitors induce activation and dual phosphorylation of the Arabidopsis thaliana MAPK 6. *J. Biol. Chem.* **275,** 7521–7526
32. Walter, H., and Larsson, C. (1994) Partitioning procedures and techniques: cells, organelles, and membranes. *Methods Enzymol.* **228,** 451–469
33. Bordier, C. (1981) Phase separation of integral membrane proteins in Triton X-114 solution. *J. Biol. Chem.* **256,** 1604–1607
34. Shevchenko, A., Wilm, M., Vorm, O., and Mann, M. (1996) Mass spectrometric sequencing of proteins silver-stained polyacrylamide gels. *Anal. Chem.* **68,** 850–858
35. Littlewood, G. M., Hooper, N. M., and Turner, A. J. (1989) Ectoenzymes of the kidney microvillar membrane. Affinity purification, characterization and localization of the phospholipase C-solubilized form of renal dipeptidase. *Biochem. J.* **257,** 361–367
36. Hooper, N. M., and Turner, A. J. (1987) Isolation of two differentially glycosylated forms of peptidyl-dipeptidase A (angiotensin converting enzyme) from pig brain: a re-evaluation of their role in neuropeptide metabolism. *Biochem. J.* **241,** 625–633
37. Bruneau, J. M., Magnin, T., Tagat, E., Legrand, R., Bernard, M., Diaquin, M., Fudali, C., and Latge, J. P. (2001) Proteome analysis of Aspergillus fumigatus identifies glycosylphosphatidylinositol-anchored proteins associated to the cell wall biosynthesis. *Electrophoresis* **22,** 2812–2823
38. Licklider, L. J., Thoreen, C. C., Peng, J., and Gygi, S. P. (2002) Automation of nanoscale microcapillary liquid chromatography-tandem mass spectrometry with a vented column. *Anal. Chem.* **74,** 3076–3083
39. Hooper, N. M., Low, M. G., and Turner, A. J. (1987) Renal dipeptidase is one of the membrane proteins released by phosphatidylinositol-specific phospholipase C. *Biochem. J.* **244,** 465–469
40. Ferguson, M. A. (1992) Site of palmitoylation of a phospholipase C-resistant glycosylphosphatidylinositol membrane anchor. *Biochem. J.* **284,** 297–300
41. Eisenhaber, F., Eisenhaber, B., Kubina, W., Maurer-Stroh, S., Neuberger, G., Schneider, G., and Wildpaner, M. (2003) Prediction of lipid posttranslational modifications and localization signals from protein sequences: big-Pi, NMT and PTS1. *Nucleic Acids Res.* **31,** 3631–3634
42. Taguchi, R., Hamakawa, N., Maekawa, N., and Ikezawa, H. (1999) Application of electrospray ionization MS/MS and matrix-assisted laser desorption/ionization-time of flight mass spectrometry to structural analysis of the glycosyl-phosphatidylinositol-anchored protein. *J. Biochem.* (*Tokyo*) **126,** 421–429
43. Iglesias, V. A., and Meins, F., Jr. (2000) Movement of plant viruses is delayed in a beta-1, 3-glucanase-deficient mutant showing a reduced plasmodesmatal size exclusion limit and enhanced callose deposition. *Plant J.* **21,** 157–166
44. Leubner-Metzger, G., and Meins, F., Jr. (2001) Antisense-transformation reveals novel roles for class I beta-1, 3-glucanase in tobacco seed after-ripening and photodormancy. *J. Exp. Bot.* **52,** 1753–1759
45. Kawamoto, T., Noshiro, M., Shen, M., Nakamasu, K., Hashimoto, K., Kawashima-Ohya, Y., Gotoh, O., and Kato, Y. (1998) Structural and phylogenetic analyses of RGD-CAP/beta ig-h3, a fasciclin-like adhesion protein expressed in chick chondrocytes. *Biochim. Biophys. Acta* **1395,** 288–292
46. Brownlee, C. (2002) Role of the extracellular matrix in cell-cell signalling: paracrine paradigms. *Curr. Opin. Plant Biol.* **5,** 396–401
47. Svetek, J., Yadav, M. P., and Nothnagel, E. A. (1999) Presence of a glycosylphosphatidylinositol lipid anchor on rose arabinogalactan proteins. *J. Biol. Chem.* **274,** 14724–14733
48. Jensen, O. N. (2004) Modification-specific proteomics: characterization of post-translational modifications of proteins. *Curr. Opin. Chem. Biol.* **8,** in press